THE JOURNAL OF PHYSICAL CHEMISTRY C

Article

pubs.acs.org/JPCC

Optical Properties of PbS/CdS Core/Shell Quantum Dots

Yolanda Justo,[*,†,∥] Pieter Geiregat,[†,‡,∥] Karen Van Hoecke,[¶] Frank Vanhaecke,[¶] Celso De Mello Donega,[§] and Zeger Hens[*,†,∥]

[†]Physics and Chemistry of Nanostructures, Ghent University, Krijgslaan 281, Building S3 (Campus Sterre), 9000 Ghent, Belgium

[‡]Photonics Research Group, Ghent University, Sint-Pietersnieuwstraat 41, 9000 Ghent, Belgium

[¶]Department of Analytical Chemistry, Ghent University, Krijgslaan 281, S12 9000 Ghent, Belgium

[§]Condensed Matter and Interfaces, Debye Institute, Utrecht University, 3508 TA Utrecht, The Netherlands

[∥]Center for Nano and Biophotonics, Ghent University, Sint-Pietersnieuwstraat 41, 9000 Gent, Belgium

Supporting Information

ABSTRACT: We determine the optical properties of PbS/CdS core/shell QDs, addressing the energy and the oscillator strength of the first exciton transition and the intrinsic absorption coefficient at short wavelengths. It follows that the intrinsic absorption coefficient at wavelengths of 350 and 400 nm agrees with theoretical numbers predicted using the Maxwell−Garnett model. Moreover, close correspondence is demonstrated between the energy and the oscillator strength of the first exciton transition of PbS/CdS core/shell and PbS QDs with a similar core size. This provides a straightforward way to estimate the PbS core diameter in PbS/CdS core/shell quantum dots by means of the PbS sizing curve, and it indicates that PbS/CdS QDs exhibit a type 1 band alignment.

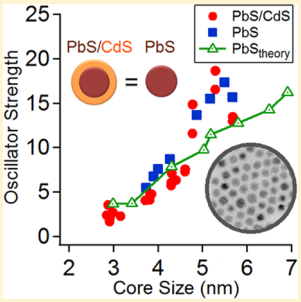

INTRODUCTION

In the field of colloidal semiconductor nanocrystals or quantum dots, overcoating initial core nanocrystals with an inorganic shell has become a standard procedure to passivate trap states at the nanocrystal surface.[1,2] When the band gap of the shell material encloses the band gap of the core, the so-called type 1 band alignment, a heterostructure develops in which the electron and hole states are confined in the core, decoupling them from possible trap states at the shell surface.[3,4] The growth of ZnS shells has been widely used in this way to increase the photoluminescence quantum yield of various nanocrystals, including II−VI quantum dots such as CdSe,[5−7] CdTe,[8] and ZnSe[9,10] and I−III−VI_2 quantum dots such as $CuInS_2$[11−13] and $CuGaS_2$.[14] Apart from slowing down nonradiative recombination pathways, it was found that shell growth also provides a means to modify the optical properties of the original core quantum dots.[15,16] In particular, the spatial separation of the electron and hole states in a core/shell quantum dot with a staggered band alignment, the so-called type 2 alignment, can lead to emission with photon energies lower than the band gap of both core and shell, respectively.[15,17−19] Moreover, the electrostatic repulsion between two excitons in such a core/shell quantum dot enabled light amplification below the threshold of one exciton per quantum dot.[20] In the intermediate case, the so-called type 1.5 behavior,[21] either the conduction or valence band of core and shell are aligned, which leads to an enhanced delocalization of the electron or the hole, respectively. In the case of CdSe/CdS heteronanostructures, it was shown that the changed overlap between electron and hole makes possible a subtle control of the fine structure of the exciton.[22,23]

In contrast to the extensive set of core/shell heteronanostructures emitting in the visible or near-infrared range (400−1000 nm), which are often based on a II−VI core quantum dot, only a limited set of heteronanostructures active at longer infrared wavelengths (1000−3000 nm) are available. Next to HgTe,[24] InAs/GaAs,[25] and InAs/InP,[26] the most widespread combination is that of a IV−VI lead chalcogenide (PbX, with X = S, Se, or Te) core quantum dot with a II−VI CdX shell. As initially demonstrated for PbSe/CdSe by Pietryga et al.,[27] these heteronanostructures can be conveniently made using cationic exchange. Although they have a different crystal structure, PbX (rock-salt) and CdX (zinc blende) share a common selenium sublattice with little mismatch between the respective lattice constants. When using relatively mild cationic exchange conditions, this allows for the formation of heteronanostructures with epitaxial interfaces as demonstrated in particular for the case of PbSe/CdSe and PbTe/CdTe quantum dots.[27,28]

Although this approach to make PbX/CdX heteronanostructures has been followed by various authors,[29−35] few studies have addressed the optical properties of PbX/CdX core/shell quantum dots. Only for the case of PbSe/CdSe QDs are extinction coefficients and a sizing curve available, allowing for the determination of the core diameter from the absorption spectrum,[36] whereas a detailed study by de Geyter et al. gave

Received: July 9, 2013
Revised: September 6, 2013
Published: September 9, 2013

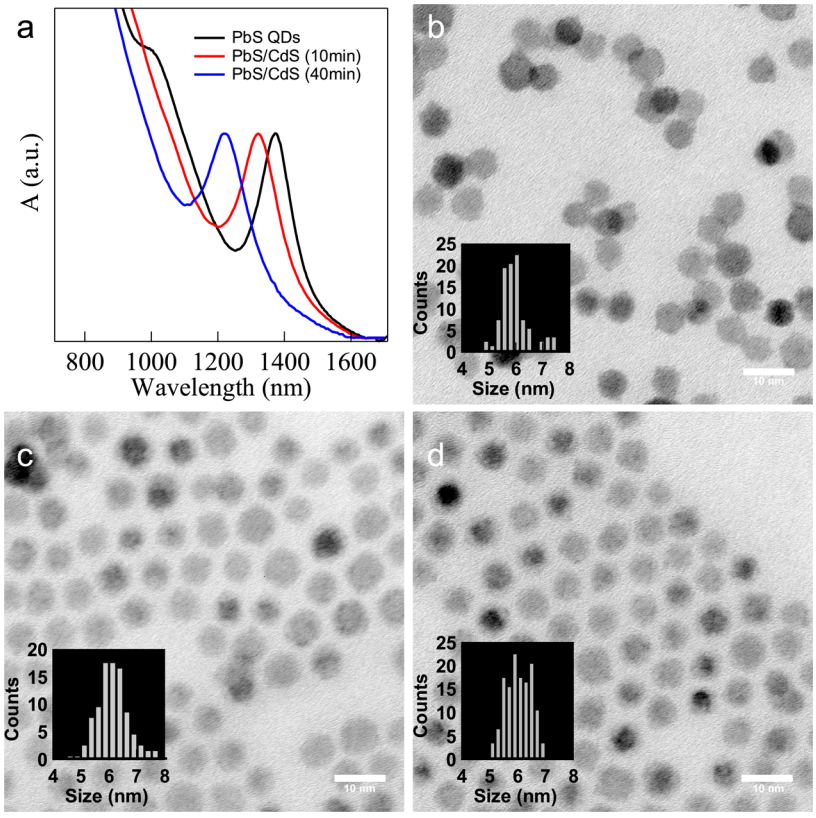

Figure 1. (a) Absorption spectra of 5.5 nm PbS QDs and the PbS/CdS core/shell QDs obtained after exposing them for 10 and 40 min to a 20-fold excess of Cd oleate at 100 °C. (b) TEM micrograph and corresponding size histogram of the PbS QDs shown in (a). (c, d) TEM micrographs and corresponding size histograms of the PbS/CdS core/shell QDs after 10 and 40 min of reaction, respectively. For all TEM micrographs, the scale bar corresponds to 10 nm.

evidence of significant electron delocalization in the shell and an enhanced splitting of the exciton fine structure.[37] In this paper, we extend this analysis to PbS/CdS core/shell quantum dots obtained using a similar cationic exchange procedure. Using elemental analysis, we find that the PbS sizing curve can be used for an accurate estimation of the PbS core diameter in PbS/CdS core/shell QDs, while the PbS/CdS absorption coefficient at short wavelengths coincides with the values predicted using the Maxwell−Garnett model in the local field approximation. We show that PbS/CdS core/shell QDs can have a photoluminescence quantum yield (PLQY) of 80% or more and show a single exponential photoluminescence decay with a lifetime in the 1−3 μs range. Using an exciton degeneracy g of 64, we obtain good agreement between the oscillator strength of the first exciton transition as calculated from the photoluminescence lifetime and the expected value for PbS QDs with the same core diameter. We thus conclude that the electronic structure of PbS and PbS/CdS QDs is highly similar, which is indicative of a type 1 band alignment in PbS/CdS core/shell QDs.

EXPERIMENTAL SECTION

Chemicals. Oleic acid (90%) and cadmium oxide (99.99%) were purchased from Sigma-Aldrich, and Oleylamine (C18-content 80−90%) was purchased from Acros Organics. Tri-*n*-octylphosphine (97%) was purchased from STREM Chemicals. Sulfur (99.999%) and $PbCl_2$ (99.999%) were purchased from Alfa-Aesar. Toluene (99.8%) and EtOH (99.9%, denaturated with 2% methyl ethyl ketone) were purchased from Fiers.

Synthesis. *PbS Synthesis.* Oleylamine (OLA)-capped PbS QDs were synthesized using a modification of the procedure developed by Cademartiri et al.[38] and described in detail in ref 39. After synthesis, the OLA ligand shell is substituted by oleic acid (OA). The QD concentration in suspension is determined from the QD absorbance spectrum using ε_{400}.[40] In the case of PbS, transmission electron microscopy (TEM) indicated the presence of a small fraction of large particles or aggregates. In that case, samples were further purified by means of size-selective precipitation using acetonitrile as a nonsolvent.

PbS/CdS Cation Exchange. PbS/CdS core/shell QDs were synthesized starting from PbS core QDs by means of a cation exchange reaction initially proposed by Pietryga et al.[27] In this reaction, an excess of cadmium oleate (0.3 M stock solution) is added to a PbS QD suspension in toluene heated to between 100 and 150 °C. After reaching the desired reaction time (between 10−300 min), the reaction is quenched using a mixture of methanol and buthanol (1:2), and the solution is purified twice. The final product is dissolved in toluene and stored under inert atmosphere.

Characterization. *Absorption Spectroscopy.* The absorbance of the colloidal solutions and thin films was determined by means of a Perkin-Elmer Lambda 950 UV−vis−NIR spectrophotometer.

Photoluminescence Spectroscopy. Photoluminescence (PL) spectra were acquired using an FS920 luminescence spectrofluorometer (Edinburgh Instruments). Samples were excited at 400 nm.

Time-Resolved Photoluminescence. Luminescence decay curves were recorded with a Spectra-Physik LPD3000 dye laser

dx.doi.org/10.1021/jp406774p | J. Phys. Chem. C 2013, 117, 20171−20177

at 480 nm pumped by a Lambda Physik LPX excimer laser. The multi-channel scaling (MCS) option integrated in the FLS920 spectrofluorometer was used to record the luminescence decay curves, using the IR-sensitive Hamamatsu R5509-72 photomultiplier tube.

ICP-OES Measurements. Inductively coupled plasma-optical emission spectrometry (ICP-OES) measurements were performed with an ICP-optical emission spectrometer with radial observation. The instrument used is a Spectro Acros (Spectro, Kleve, Germany). Concentrations of Pb and Cd were determined in 15 mL solutions prepared following the procedure described in the Supporting Information. Two or three emission lines per element were monitored in the analysis.

Size Determination. The mean diameter of the PbS and PbS/CdS QDs was determined from bright-field TEM images recorded with a Cs-corrected JEM-2200FS transmission electron microscope. The samples for TEM were prepared by drop casting a diluted suspension of QDs on holey carbon film supported by a copper TEM grid. On the basis of the TEM images, the size histograms and mean diameter of the QDs are determined by analyzing 100−150 particles for each sample.

RESULTS AND DISCUSSION

PbS Core Size Determination. As reported by Pietryga et al.,[27] exposing a dispersion of PbS QDs to cadmium oleate at temperatures in the range of 100−150 °C initiates a cationic exchange process where lead cations are replaced by cadmium, thus forming a PbS/CdS core/shell heterostructure. Taking the example of 5.7 nm core PbS QDs exposed to a 20-fold excess of cadmium oleate at 100 °C, Figure 1a shows that the growth of a CdS shell, and the concomitant reduction of the PbS core, leads to a gradual blue shift of the peak wavelength λ_{1S-1S} of the first exciton transition. Importantly, in agreement with various literature reports,[28,31] the cationic exchange leaves the overall diameter of the nanocrystals unchanged. According to TEM analysis, the average diameter of the nanocrystals changes from 5.6 to 5.9 nm after a 40 min cationic exchange reaction under the conditions used in Figure 1, which is well within the uncertainty of the diameter determined by TEM.

Knowledge of the core diameter and shell thickness is essential to a detailed quantification of the opto-electronic properties of the core/shell QDs.[37,41] As the first exciton transition in PbS/CdS core/shell QDs still shows a well-defined, albeit broadened, absorption peak, we will at first look for a relation between the peak wavelength λ_{1S-1S} and the core diameter. Such a sizing curve is typically used to determine the diameter of core QDs, and in the particular case of PbSe/CdSe QDs, it has been shown that the PbSe core diameter can be estimated using the sizing curve of PbSe QDs.[36]

To estimate the average diameter of the PbS core in PbS/CdS core/shell QDs, we determined the amount of Cd and Pb (N_{Cd} and N_{Pb}, respectively) in various samples of PbS/CdS QDs using ICP-OES. These numbers enable the calculation of the total volume of CdS (V_{CdS}) and PbS (V_{PbS}) in the sample (see Supporting Information):

$$V_{CdS} = \frac{a_{CdS}^3}{4} N_{Cd} \quad (1)$$

$$V_{PbS} = \frac{a_{PbS}^3}{8} N_{Pb} + \frac{a_{PbS}^3}{8} \frac{N_{Pb} - 0.2N_{Cd}}{1.2} \quad (2)$$

Here, a_{CdS} and a_{PbS} denote the lattice constant of CdS and PbS, respectively. To arrive at eqs 1 and 2, we have assumed that the CdS shell is stoichiometric, while the PbS core is not, with a Pb:S ratio of 1.2.[40] Having the average volume of CdS and PbS in each core/shell QD and the core/shell diameter D and regarding PbS/CdS core/shell QDs as consisting of a spherical PbS core centered within an overall spherical nanocrystal (see Figure 2a), a core diameter d_{ICP} can be calculated as

$$d_{ICP} = \left(\frac{V_{PbS}}{V_{CdS} + V_{PbS}} \right)^{1/3} D \quad (3)$$

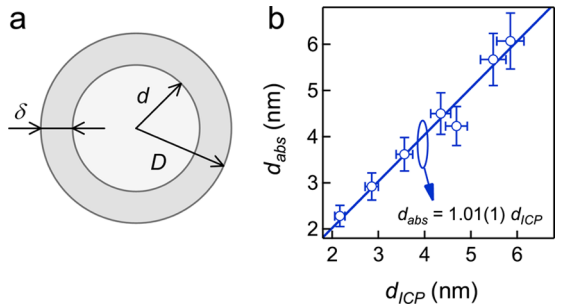

Figure 2. (a) Representation of the concentric, spheric core/shell model used to derive core diameter and shell thickness from the elemental analysis data, with an indication of core diameter (d), nanocrystal diameter (D), and shell thickness (δ). (b) Comparison of the PbS core diameter as determined from the peak wavelength of the first exciton transition in the UV−vis spectrum (d_{abs}) and the PbS core diameter as determined using elemental analysis (d_{ICP}).

An alternative estimation of the core diameter is obtained by applying the PbS sizing curve to the peak wavelength λ_{1S-1S} of the first exciton transition of PbS/CdS core/shell QDs.[40] In Figure 2b, we compare the thus obtained core diameter d_{abs} with d_{ICP}, i.e., the core diameter as obtained by applying eq 3. The figure shows that both diameters are directly proportional, with a best-fitting line yielding a slope of 1.01(1). We thus conclude that the PbS core diameter of PbS/CdS QDs can be determined from the peak wavelength of the first exciton transition using the PbS sizing curve. This conclusion is in agreement with a study on PbSe/CdSe QDs,[37] yet it contradicts previous finding on PbS/CdS core/shell QDs.[31]

Absorption Coefficient of PbS/CdS Quantum Dots. The intrinsic absorption coefficient μ_i is a most convenient quantity to describe light absorption by a dilute dispersion of nanocrystals.[36,42] It relates the volume fraction f of the QDs in dispersion, i.e., the ratio between the volume of the QDs and the total volume of the dispersion, to the absorbance A of that dispersion. With L the length of the optical path through the sample, μ_i is defined as

$$\mu_i = \frac{A \ln(10)}{fL} \quad (4)$$

In the case of point-like, dispersed spherical particles at low volume fractions, the Maxwell−Garnett effective medium theory provides an expression for μ_i that depends only on the dielectric function of the particles ($\tilde{\varepsilon} = \varepsilon_R + i\varepsilon_I$) and the surroundings ($\varepsilon_s$):

dx.doi.org/10.1021/jp406774p | J. Phys. Chem. C 2013, 117, 20171−20177

$$\mu_i = \frac{2\pi}{\lambda n_s}\left|\frac{3\varepsilon_s}{\tilde{\varepsilon} + 2\varepsilon_s}\right|^2 \varepsilon_I \quad (5)$$

For various core QDs, it has been demonstrated that the experimentally determined intrinsic absorption coefficient at short wavelengths coincides with a theoretical value obtained using the dielectric function of the bulk material in eq 5. For core/shell QDs, a similar expression for the intrinsic absorption coefficient has been proposed by Neeves et al.,[43] where the indices c and s refer to core and shell, respectively:

$$\mu_i = \frac{2\pi}{\lambda n_s}\mathrm{Im}(3\varepsilon_s\beta)$$

$$\text{with } \beta = \left(\frac{\varepsilon_s\varepsilon_a - \varepsilon_s\varepsilon_b}{\varepsilon_s\varepsilon_a + 2\varepsilon_s\varepsilon_b}\right)$$

$$\varepsilon_a = \varepsilon_c\left(3 - 2\frac{V_s}{V_{tot}}\right) + 2\varepsilon_s\frac{V_s}{V_{tot}}$$

$$\varepsilon_b = \varepsilon_c\frac{V_s}{V_{tot}} + \varepsilon_s\left(3 - \frac{V_s}{V_{tot}}\right) \quad (6)$$

This expression shows that in the case of core/shell QDs, μ_i depends on V_s/V_{tot}, i.e., the ratio between the shell volume and the total QD volume, and on the dielectric functions of the core (ε_c), shell (ε_S), and surroundings. In the case of PbSe/CdSe QDs, close agreement was demonstrated between the experimental μ_i at short wavelengths and a theoretical value calculated using the bulk dielectric function of the core and shell in eq 6.

For all samples analyzed using ICP-OES, we can calculate the volume fraction of PbS/CdS core/shell QDs, assuming a stoichiometric CdS shell and a nonstoichiometric core with a Pb:S ratio of 1.2:1. Combining the resulting value with the absorbance of these dispersions, we arrive at experimental values for the intrinsic absorption coefficient. The resulting numbers are represented in Figure 3 as a function of the ratio of the shell volume to the total QD volume (V_s/V_{tot}) at wavelengths of 400 and 350 nm. Next to the experimental μ_i, the full lines in Figure 3 represent values obtained through eq 6 when using the dielectric function of the bulk PbS and CdS for core and shell, respectively.[44,45] Similar to PbSe/CdSe, a good agreement is obtained between these theoretical values and the experimental data based on ICP-OES analysis. We therefore recommend using these calculated intrinsic absorption coefficients as a function of V_s/V_{tot} to calculate the volume fraction and thus the concentration of dispersed PbS/CdS core/shell QDs. Tabulated values at 400 and 350 nm can be found in the Supporting Information.

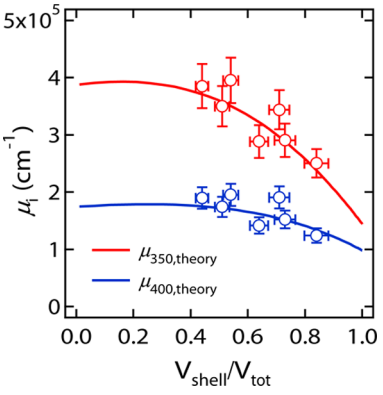

Figure 3. Intrinsic absorption coefficient as obtained at (red circles) 350 nm and (blue circles) 400 nm for PbS/CdS core/shell QDs in C_2Cl_4. The full lines represent theoretical absorption coefficients calculated using the bulk dielectric function of PbS and CdS at the respective wavelengths.

The Oscillator Strength of the First Exciton Transition. Figure 4a shows the absorption and emission spectra of 5.7 nm PbS QDs and two samples of PbS/CdS core/shell QDs made from it using cationic exchange at different temperatures and different times. One clearly sees that the photoluminescence follows both the blueshift and the broadening of the first exciton absorption feature. For various PbS/CdS QDs, we determined the photoluminescence quantum yield (PLQY) using an integrating sphere.[46] As indicated in Figure 4b, PbS/CdS QDs can have a very high PLQY. Especially for smaller cores, the PLQY typically exceeds 60%, with a few samples having values above 80 and 90%. As was reported for the starting core PbS QDs,[39] the QY shows a large sample-to-sample difference, yet it tends to go down with increasing core size. In addition, no marked difference is observed with the PLQY of the original PbS core QDs.

Figure 4c shows a typical photoluminescence decay curve for PbS/CdS QDs after excitation with a pulsed dye laser at 480 nm. In contrast to PbSe/CdSe QDs,[37] the decay can be satisfactorily described using a single exponential fit, yielding the luminescent lifetime τ_{PL}. The τ_{PL} of several samples of PbS and PbS/CdS QDs thus obtained is plotted as a function of the PbS core diameters in Figure 4d. Typical values range between 1 and 3 μs, where for both PbS and PbS/CdS QDs we find that smaller cores yield longer lifetimes, while no clear difference in lifetime emerges between PbS and PbS/CdS QDs. Importantly, τ_{PL} as represented in Figure 4d is the lifetime obtained by fitting the photoluminescent decay using a single exponential, i.e., without correcting for differences in quantum yield. If the measured quantum yield of the QD ensemble corresponds to that of each individual QD (homogeneous sample), the radiative lifetime τ_{rad} can be obtained by dividing τ_{PL} by the PLQY. As shown in the Supporting Information, the data set shown in Figure 4d contains data measured on similar quantum dots with considerably different quantum yields. As a result, calculating τ_{rad} as τ_{PL}/PLQY results in considerable outliers, while τ_{PL} itself yields a consistent trend with the PbS core size. We therefore conclude that in this case the monoexponential fit to the photoluminescent decay directly yields the radiative lifetime, i.e., $\tau_{PL} = \tau_{rad}$. This could point toward sample heterogeneity, where a fraction of the QDs is dark while the others emit with a 100% quantum yield, resulting in a PLQY lower than 100% with a PL decay curve still yielding the radiative lifetime.

The radiative lifetime τ_{rad} of the first exciton transition is related to the oscillator strength f_{1S-1S} of this transition. Assuming a g-fold degenerate first exciton where all the fine structure levels are equally accessible through thermal excitations, f_{1S-1S} is obtained as[42]

$$f_{1S-1S} = \frac{2\pi\varepsilon_0 c^3 m_e}{e^2}\frac{g}{n_s|f_{LF}|^2\omega^2}\tau_{rad}^{-1} \quad (7)$$

Here, $|f_{LF}|^2$ denotes the amplitude square of the so-called local field factor, which describes the screening of the PbS core by

dx.doi.org/10.1021/jp406774p | J. Phys. Chem. C 2013, 117, 20171−20177

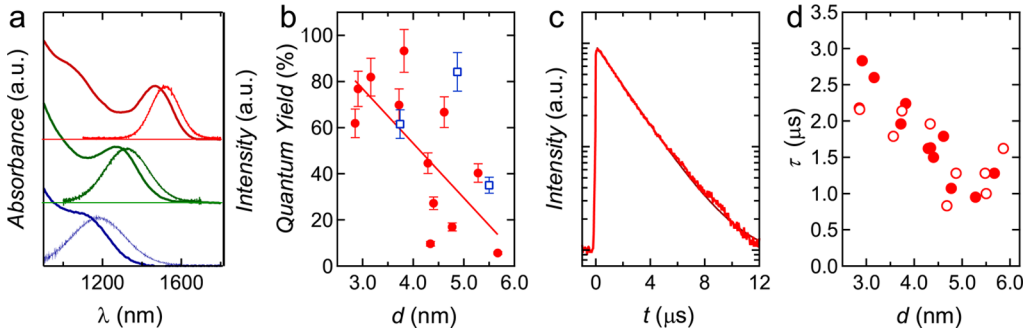

Figure 4. (a) Absorption and emission spectra of 5.7 nm PbS QDs (red) and PbS/CdS core/shell QDs with 0.5 nm shells (green) and 0.8 nm shells (blue). The graph shows the blue shift of the absorption and emission peaks due to the shrinkage of the PbS core. (b) Photoluminescence quantum yield as a function of the PbS core diameter for PbS/CdS core/shell QDs (filled red circles) and PbS QDs (empty blue squares). Horizontal error bars omitted for clarity. The uncertainty on the determination of the diameter is estimated to be 10%. (c) Typical photoluminescence decay curve for a PbS/CdS core/shell QD shown on a logarithmic scale with a single exponential fit (black line). (d) Luminescent lifetime as a function of PbS core diameter for PbS QDs (empty red circles) and PbS/CdS core/shell QDs (filled red circles). The standard error did not exceed 1% for all samples measured. Horizontal error bars omitted for clarity. The uncertainty on the determination of the diameter is estimated to be 10%.

the CdS shell and the solvent (see Supporting Information).[43] In Figure 5, we plot f_{1S-1S} calculated for PbS/CdS QDs

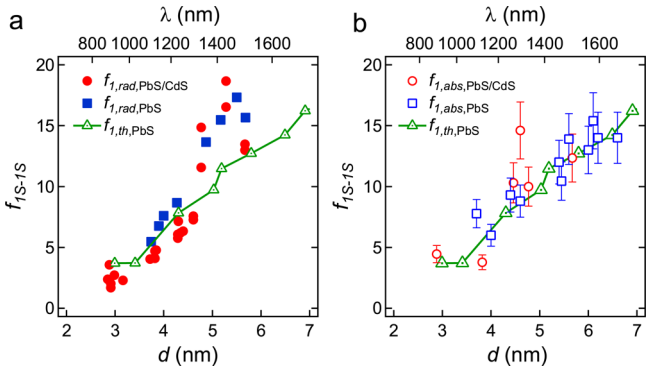

Figure 5. Oscillator strength f_{1S-1S} of the band-edge transition of PbS (blue squares) and PbS/CdS (red circles) QDs as a function of particle size and wavelength obtained from the radiative lifetime (a) and the spectrum of the intrinsic absorption coefficient (b). Standard error is below 1% at all data points. In both cases, the values are compared with theoretical predictions taken from ref 40 (green triangles). Horizontal error bars are omitted for clarity. The uncertainty in the determination of the diameter is estimated to be 10%.

according to eq 7, assuming $g = 64$. The resulting numbers are compared with figures obtained similarly for PbS QDs and with the oscillator strength of the PbS first exciton transition as calculated using tight binding methods.[40] Although f_{1S-1S} as derived from the luminescent lifetime for PbS/CdS tends to be somewhat smaller than that for PbS QDs, both agree reasonably well with the predicted value for PbS QDs for core diameters smaller than 5 nm. For larger QDs, the f_{1S-1S} values as obtained from the luminescent lifetime tend to exceed the theoretical oscillator strength, which means that the measured τ_{PL} becomes shorter than the predicted radiative lifetime. In line with the overall reduction of the PLQY with increasing diameter, this may indicate that the exciton recombination rate is increased by the opening up of an additional nonradiative decay channel for these larger QDs. In fact, the wavelength range where this deviation is observed ($\lambda >$ 1300 nm) is in reasonable agreement with the observation, in the case of PbSe QDs, that energy transfer to surface ligands reduces the exciton lifetime and lowers the PLQY at wavelengths above 1600 nm.[47]

Alternatively, f_{1S-1S} can also be obtained from the spectrum of the intrinsic absorption coefficient by integrating μ_i over the first exciton peak and including the obtained value, called $\mu_{i,gap}$, in the following expression:[48]

$$f_{if,abs} = \frac{2\varepsilon_0 c m_e n_s}{e\pi\hbar} \frac{V_{QD}}{|f_{LF}|^2} \mu_{i,gap} \quad (8)$$

Because of the significant broadening of the first exciton peak during the cationic exchange, we determined $\mu_{i,gap}$ by fitting the absorption spectra around the first exciton transition using the sum of a Gaussian and a polynomial background (see Supporting Information). The values obtained in this manner are depicted in Figure 5b, where we represented only those points for PbS/CdS for which a reliable background correction proved possible. One can see that the resulting oscillator strength for both PbS/CdS core/shell and PbS core QDs values follows the trend of the PbS QDs values obtained using tight binding calculations.

Given the correspondence between both the energy and the oscillator strength of the band gap transition of PbS/CdS core/shell and PbS QDs with the same core diameter, it follows that the room-temperature properties of this transition are not affected by CdS shell growth. This indicates that PbS/CdS core/shell QDs have a type 1 band alignment, in which the bands of the PbS core are contained within those of the CdS shell.

CONCLUSIONS

We have analyzed the optical properties of PbS/CdS core/shell QDs by means of UV−vis absorption and photoluminescence spectroscopy, time-resolved photoluminescence, and ICP-OES measurements. The results show, as for PbSe/CdSe QDs, that the PbS sizing curve can be used to estimate the diameter of the core and therefore to obtain the shell thickness. The intrinsic absorption coefficient, predicted using the Maxwell−Garnett model and calculated as a function of V_s/V_{tot}, coincides with that of the experimental samples whose f has been obtained by ICP-OES. Therefore, we can use $\mu_{400,th}$ as a function of V_s/V_{tot} to calculate the volume fraction or the concentration of dispersed PbS/CdS core/shell QDs. Regarding the time-resolved PL for PbS and PbS/CdS QDs, smaller cores yield

dx.doi.org/10.1021/jp406774p | J. Phys. Chem. C 2013, 117, 20171−20177

longer lifetimes, with typical values ranging between 1 and 3 μs. The oscillator strength of the PbS/CdS band gap transition, calculated from either the spectrum of the intrinsic absorption coefficient or the radiative lifetime, corresponds to that of PbS QDs and agrees with numbers calculated for PbS QDs using tight binding calculations. On the basis of this close agreement between the optical properties of the band gap transition of PbS/CdS core/shell and PbS core QDs, we conclude that PbS/CdS QDs exhibit a type 1 band alignment.

■ ASSOCIATED CONTENT

Supporting Information

A summary of the ICP-OES results, $\mu_{350,th}$ and $\mu_{400,th}$ values as a function of V_s/V_{tot}, additional time-resolved PL measurements, a mathematical expression for $|f_{LF}|^2$, and a description of the absorption background correction material. This material is available free of charge via the Internet at http://pubs.acs.org.

■ AUTHOR INFORMATION

Corresponding Authors

*E-mail: Yolanda.Justo@UGent.be.
*E-mail: Zeger.Hens@UGent.be.

Notes

The authors declare no competing financial interest.

■ ACKNOWLEDGMENTS

This research has been funded by the FWO-Vlaanderen (project NanoMIR), BelSPo (IAP 7.35, photonics@be), and EU-FP7 (ITN Herodot, Grant Agreement 214954, STREP Navolchi).

■ REFERENCES

(1) Kim, M. R.; Chung, J. H.; Lee, M.; Lee, S.; Jang, D.-J. Fabrication, Spectroscopy, and Dynamics of Highly Luminescent Core-Shell InP@ZnSe Quantum Dots. *J. Colloid Interface Sci.* **2010**, *350*, 5−9.

(2) Zhang, Y.; Dai, Q. Q.; Li, X. B.; Cui, Q. Z.; Gu, Z. Y.; Zou, B.; Wang, Y. D.; Yu, W. W. Formation of PbSe/CdSe Core/Shell Nanocrystals for Stable Near-Infrared High Photoluminescence Emission. *Nanoscale Res. Lett.* **2010**, *5*, 1279−1283.

(3) Dorfs, D.; Franzl, T.; Osovsky, R.; Brumer, M.; Lifshitz, E.; Klar, T. A.; Eychmüller, A. Type-I and Type-II Nanoscale Heterostructures Based on CdTe Nanocrystals: A Comparative Study. *Small* **2008**, *4*, 1148−52.

(4) Zhu, Z.; Ouyang, G.; Yang, G. The Interface Effect on the Band Offset of Semiconductor Nanocrystals with Type-I Core-Shell Structure. *Phys. Chem. Chem. Phys.* **2013**, *15*, 5472−6.

(5) Hines, M. A.; Guyot-Sionnest, P. Synthesis and Characterization of Strongly Luminescing ZnS-Capped CdSe Nanocrystals. *J. Phys. Chem.* **1996**, *100*, 468−471.

(6) Dabbousi, B. O.; RodriguezViejo, J.; Mikulec, F. V.; Heine, J. R.; Mattoussi, H.; Ober, R.; Jensen, K. F.; Bawendi, M. G. (CdSe)ZnS Core−Shell Quantum Dots: Synthesis and Characterization of a Size Series of Highly Luminescent Nanocrystallites. *J. Phys. Chem. B* **1997**, *101*, 9463−9475.

(7) Dethlefsen, J. R.; Døssing, A. Preparation of a ZnS Shell on CdSe Quantum Dots using a Single-Molecular ZnS Precursor. *Nano Lett.* **2011**, *11*, 1964−9.

(8) Tsay, J. M.; Pflughoefft, M.; Bentolila, L. A.; Weiss, S. Hybrid Approach to the Synthesis of Highly Luminescent CdTe/ZnS and CdHgTe/ZnS Nanocrystals. *J. Am. Chem. Soc.* **2004**, *126*, 1926−7.

(9) Wu, Y.; Arai, K.; Yao, T. Temperature Dependence of the Photoluminescence of ZnSe/ZnS Quantum-Dot Structures. *Phys. Rev. B* **1996**, *53*, R10485−R10488.

(10) Nikesh, V. V.; Mahamuni, S. Highly Photoluminescent ZnSe/ZnS. *Semicond. Sci. Technol.* **2001**, *16*, 687−690.

(11) Trizio, L. D.; Prato, M.; Genovese, A.; Casu, A.; Povia, M.; Simonutti, R.; Alcocer, M. J. P.; Andrea, C. D.; Tassone, F.; Manna, L. Strongly Fluorescent Quaternary Cu−In−Zn−S Nanocrystals Prepared from $Cu_{1-x}InS_2$ Nanocrystals by Partial Cation Exchange. *Chem. Mater.* **2012**, *24*, 2400−2406.

(12) Song, W.-S.; Yang, H. Efficient White-Light-Emitting Diodes Fabricated from Highly Fluorescent Copper Indium Sulfide Core/Shell Quantum Dots. *Chem. Mater.* **2012**, *24*, 1961−1967.

(13) Jang, E.-P.; Song, W.-S.; Lee, K.-H.; Yang, H. Preparation of a Photo-Degradation-Resistant Quantum Dot-Polymer Composite Plate for use in the Fabrication of a High-Stability White-Light-Emitting Diode. *Nanotechnology* **2013**, *24*, 045607.

(14) Song, W.-S.; Kim, J.-H.; Lee, J.-H.; Lee, H.-S.; Do, Y. R.; Yang, H. Synthesis of Color-Tunable Cu−In−Ga−S Solid Solution Quantum Dots with High Quantum Yields for Application to White Light-Emitting Diodes. *J. Mater. Chem.* **2012**, *22*, 21901.

(15) Kim, S.; Fisher, B.; Eisler, H.-J.; Bawendi, M. Type-II Quantum Dots: CdTe/CdSe(Core/Shell) and CdSe/ZnTe(Core/Shell) Heterostructures. *J. Am. Chem. Soc.* **2003**, *125*, 11466−7.

(16) Balet, L. P.; Ivanov, S. A.; Piryatinski, A.; Achermann, M.; Klimov, V. I. Inverted Core/Shell Nanocrystals Continuously Tunable between Type-I and Type-II Localization Regimes. *Nano Lett.* **2004**, *4*, 1485−1488.

(17) Zeng, Q. H.; Kong, X. G.; Sun, Y. J.; Zhang, Y. L.; Tu, L. P.; Zhao, J. L.; Zhang, H. Synthesis and Optical Properties of Type II CdTe/CdS Core/Shell Quantum Dots in Aqueous Solution via Successive Ion Layer Adsorption and Reaction. *J. Phys. Chem. C* **2008**, *112*, 8587−8593.

(18) Dennis, A. M.; Mangum, B. D.; Piryatinski, A.; Park, Y.-S.; Hannah, D. C.; Casson, J. L.; Williams, D. J.; Schaller, R. D.; Htoon, H.; Hollingsworth, J. A. Suppressed Blinking and Auger Recombination in Near-Infrared Type-II InP/CdS Nanocrystal Quantum Dots. *Nano Lett.* **2012**, *12*, 5545−51.

(19) Nemchinov, A.; Kirsanova, M.; Hewa-Kasakarage, N. N.; Zamkov, M. Synthesis and Characterization of Type II ZnSe/CdS Core/Shell Nanocrystals. *J. Phys. Chem. C* **2008**, *112*, 9301−9307.

(20) Klimov, V. I.; Ivanov, S. A.; Nanda, J.; Achermann, M.; Bezel, I.; McGuire, J. A.; Piryatinski, A. Single-Exciton Optical Gain in Semiconductor Nanocrystals. *Nature* **2007**, *447*, 441−6.

(21) de Mello Donegá, C. Synthesis and properties of colloidal heteronanocrystals. *Chem. Soc. Rev.* **2011**, *40*, 1512−46.

(22) Rainò, G.; Stöferle, T.; Moreels, I.; Gomes, R.; Hens, Z.; Mahrt, R. F. Controlling the Exciton Fine Structure Splitting in CdSe/CdS Dot-in-Rod Nanojunctions. *ACS Nano* **2012**, *6*, 1979−87.

(23) Shabaev, A.; Rodina, A. V.; Efros, A. L. Fine Structure of the Band-Edge Excitons and Trions in CdSe/CdS Core/Shell Nanocrystals. *Phys. Rev. B* **2012**, *86*, 205311.

(24) Keuleyan, S.; Lhuillier, E.; Guyot-Sionnest, P. Synthesis of Colloidal HgTe Quantum Dots for Narrow Mid-IR Emission and Detection. *J. Am. Chem. Soc.* **2011**, *133*, 16422−4.

(25) Harris, L.; Mowbray, D. J.; Skolnick, M. S.; Hopkinson, M.; Hill, G. Emission Spectra and Mode Structure of InAs/GaAs Self-Organized Quantum Dot Lasers. *Appl. Phys. Lett.* **1998**, *73*, 969.

(26) Cao, Y.-W.; Banin, U. Synthesis and Characterization of InAs/InP and InAs/CdSe Core/Shell Nanocrystals. *Angew. Chem., Int. Ed.* **1999**, *38*, 3692−3694.

(27) Pietryga, J. M.; Werder, D. J.; Williams, D. J.; Casson, J. L.; Schaller, R. D.; Klimov, V. I.; Hollingsworth, J. A. Utilizing the Lability of Lead Selenide to Produce Heterostructured Nanocrystals with Bright, Stable Infrared Emission. *J. Am. Chem. Soc.* **2008**, *130*, 4879−4885.

(28) Lambert, K.; De Geyter, B.; Moreels, I.; Hens, Z. PbTe|CdTe Core|Shell Particles by Cation Exchange, a HR-TEM study. *Chem. Mater.* **2009**, *21*, 778−780.

(29) Neo, M. S.; Venkatram, N.; Li, G. S.; Chin, W. S.; Ji, W. Synthesis of PbS/CdS Core−Shell QDs and their Nonlinear Optical Properties. *J. Phys. Chem. C* **2010**, *114*, 18037−18044.

(30) Wheeler, D. A.; Fitzmorris, B. C.; Zhao, H.; Ma, D.; Zhang, J. Ultrafast Exciton Relaxation Dynamics of PbS and Core/Shell PbS/CdS Quantum Dots. *Sci. China, Ser. B: Chem.* **2011**, *54*, 2009−2015.
(31) Zhao, H.; Chaker, M.; Wu, N.; Ma, D. Towards Controlled Synthesis and Better Understanding of Highly Luminescent PbS/CdS Core/Shell Quantum Dots. *J. Mater. Chem.* **2011**, *21*, 8898−8904.
(32) Zhang, Y.; Dai, Q. Q.; Li, X. B.; Cui, Q. Z.; Gu, Z. Y.; Zou, B.; Wang, Y. D.; Yu, W. W. Formation of PbSe/CdSe Core/Shell Nanocrystals for Stable Near-Infrared High Photoluminescence Emission. *Nanoscale Res. Lett.* **2010**, *5*, 1279−1283.
(33) Abel, K. A.; Qiao, H.; Young, J. F.; van Veggel, F. C. J. M. Four-Fold Enhancement of the Activation Energy for Nonradiative Decay of Excitons in PbSe/CdSe Core/Shell versus PbSe Colloidal Quantum Dots. *J. Phys. Chem. Lett.* **2010**, *1*, 2334−2338.
(34) Xu, T.; Wu, H.; Si, J.; McCann, P. Optical Transitions in PbTe/CdTe Quantum Dots. *Phys. Rev. B* **2007**, *76*, 155328.
(35) Groiss, H.; Kaufmann, E.; Springholz, G.; Schwarzl, T.; Hesser, G.; Schäffler, F.; Heiss, W.; Koike, K.; Itakura, T.; Hotei, T.; et al. Size Control and Midinfrared Emission of Epitaxial PbTe/CdTe Quantum Dot Precipitates Grown by Molecular Beam Epitaxy. *Appl. Phys. Lett.* **2007**, *91*, 222106.
(36) Geyter, B. D.; Hens, Z. The Absorption Coefficient of PbSe/CdSe Core/Shell Colloidal Quantum Dots. *Appl. Phys. Lett.* **2010**, *97*, 161908.
(37) De Geyter, B.; Justo, Y.; Moreels, I.; Lambert, K.; Smet, P. F.; Van Thourhout, D.; Houtepen, A. J.; Grodzinska, D.; de Mello Donega, C.; Meijerink, A.; et al. The Different Nature of Band Edge Absorption and Emission in Colloidal PbSe/CdSe Core/Shell Quantum Dots. *ACS Nano* **2011**, *5*, 58−66.
(38) Cademartiri, L.; Bertolotti, J.; Sapienza, R.; Wiersma, D. S.; von Freymann, G.; Ozin, G. A. Multigram Scale, Solventless, and Diffusion-Controlled Route to Highly Monodisperse PbS Nanocrystals. *J. Phys. Chem. B* **2006**, *110*, 671−3.
(39) Moreels, I.; Justo, Y.; De Geyter, B.; Haustraete, K.; Martins, J. C.; Hens, Z. Size-Tunable, Bright, and Stable PbS Quantum Dots: A Surface Chemistry Study. *ACS Nano* **2011**, *5*, 2004−2012.
(40) Moreels, I.; Lambert, K.; Smeets, D.; De Muynck, D.; Nollet, T.; Martins, J. C. J. C.; Vanhaecke, F.; Vantomme, A. A.; Delerue, C.; Allan, G.; et al. Size-Dependent Optical Properties of Colloidal PbS Quantum Dots. *ACS Nano* **2009**, *3*, 3023−3030.
(41) Nguyen, T.; Habinshuti, J.; Justo, Y.; Gomes, R.; Mahieu, G.; Godey, S.; Nys, J.; Carrillo, S.; Hens, Z.; Robbe, O.; et al. Charge Carrier Identification in Tunneling Spectroscopy of Core-Shell Nanocrystals. *Phys. Rev. B* **2011**, *84*, 1−8.
(42) Hens, Z.; Moreels, I. Light Absorption by Colloidal Semiconductor Quantum Dots. *J. Mater. Chem.* **2012**, *22*, 10406.
(43) Neeves, A.; Birnboim, M. Composite Structures for the Enhancement of Nonlinear-Optical Susceptibility. *J. Opt. Soc. Am. B* **1989**, *6*, 787−796.
(44) Suzuki, N.; Sawai, K.; Adachi, S. Optical Properties of PbSe. *J. Appl. Phys.* **1995**, *77*, 1249−1255.
(45) Ninomiya, S.; Adachi, S. Optical Properties of Cubic and Hexagonal CdSe. *J. Appl. Phys.* **1995**, *78*, 4681−4689.
(46) Porrès, L.; Holland, A.; Pålsson, L.-O.; Monkman, A. P.; Kemp, C.; Beeby, A. Absolute Measurements of Photoluminescence Quantum Yields of Solutions Using an Integrating Sphere. *J. Fluoresc.* **2006**, *16*, 267−72.
(47) Liu, H.; Guyot-Sionnest, P. Photoluminescence Lifetime of Lead Selenide Colloidal Quantum Dots. *J. Phys. Chem. C* **2010**, *114*, 14860−14863.
(48) Moreels, I.; Lambert, K.; De Muynck, D.; Vanhaecke, F.; Poelman, D.; Martins, J. C.; Allan, G.; Hens, Z. Composition and Size-Dependent Extinction Coefficient of Colloidal PbSe Quantum Dots. *Chem. Mater.* **2007**, *19*, 6101−6106.